

Supplementary information

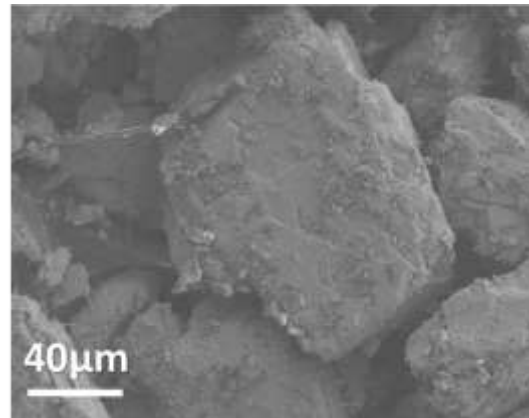
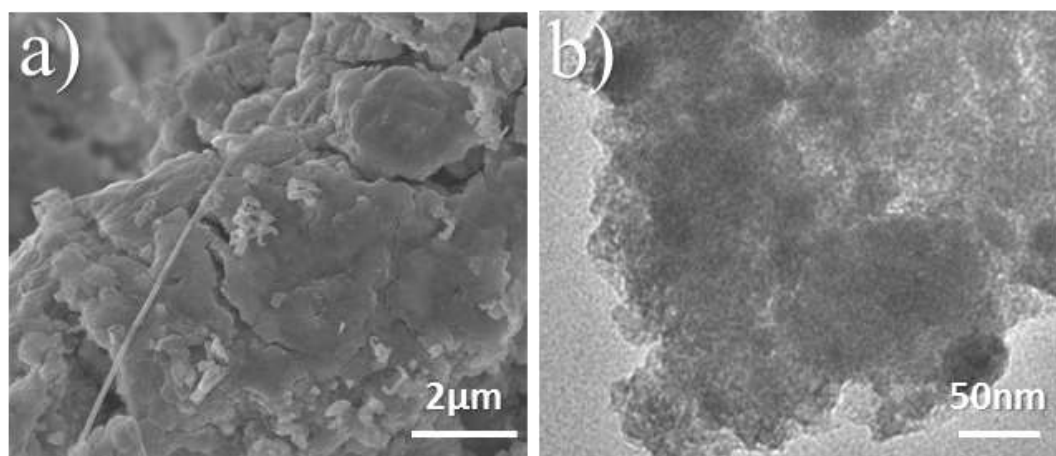


Figure S1. An SEM image of as-melted YSn_2 .



FigureS2. a) An SEM image, b) a TEM image of $\text{YSn}_2\text{-Ar}$.

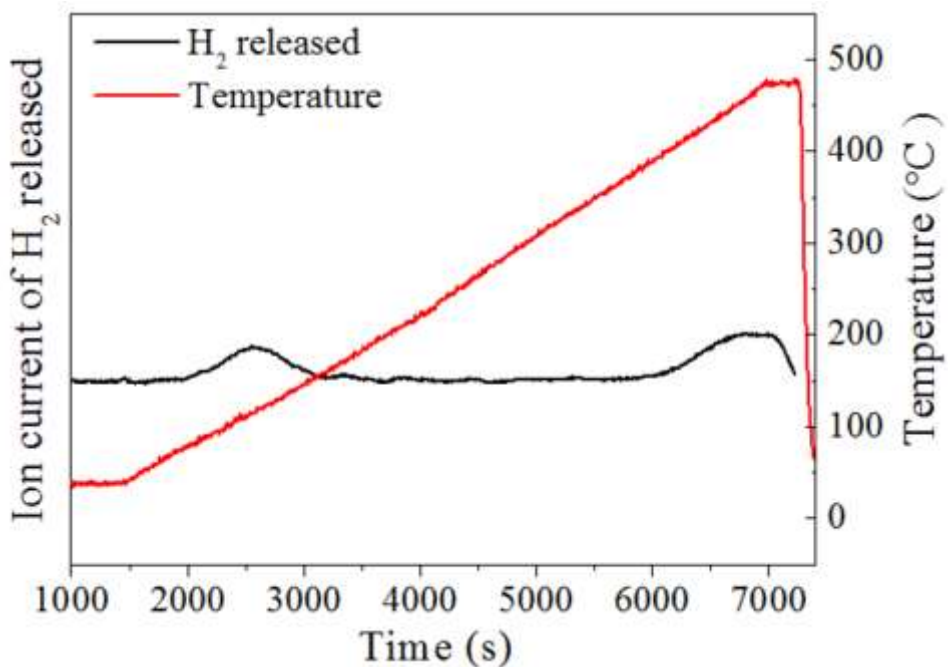


Figure S3. The curves of TPD-MS of dehydrogenation process of Sn/YH_x

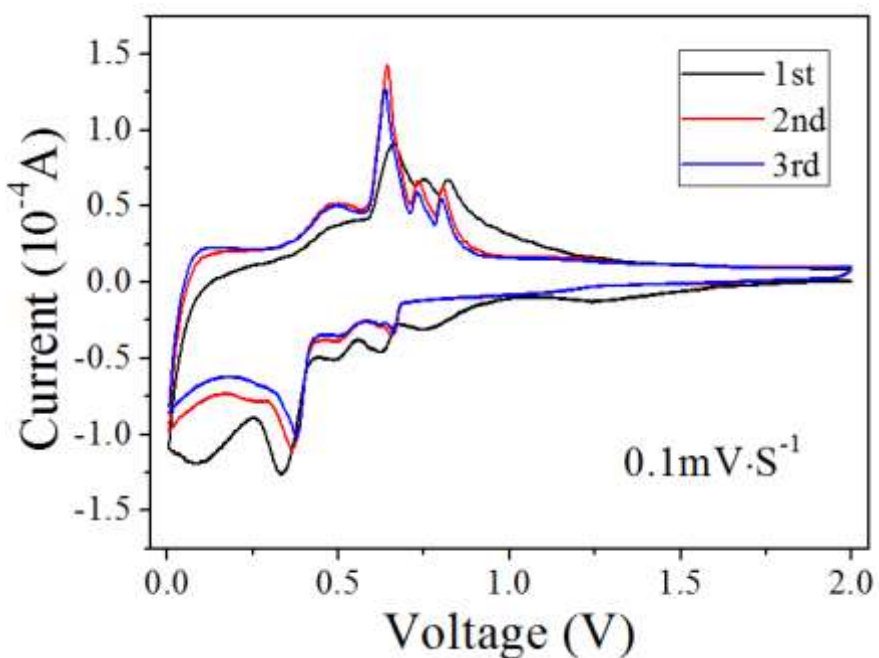
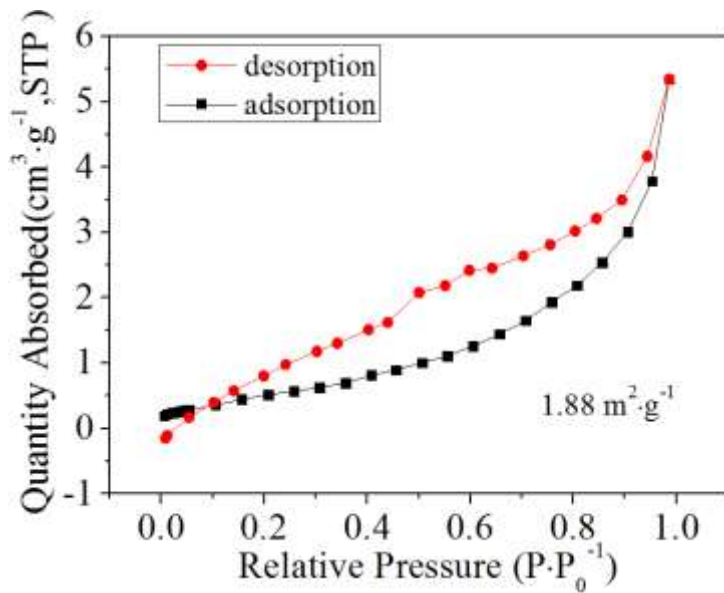
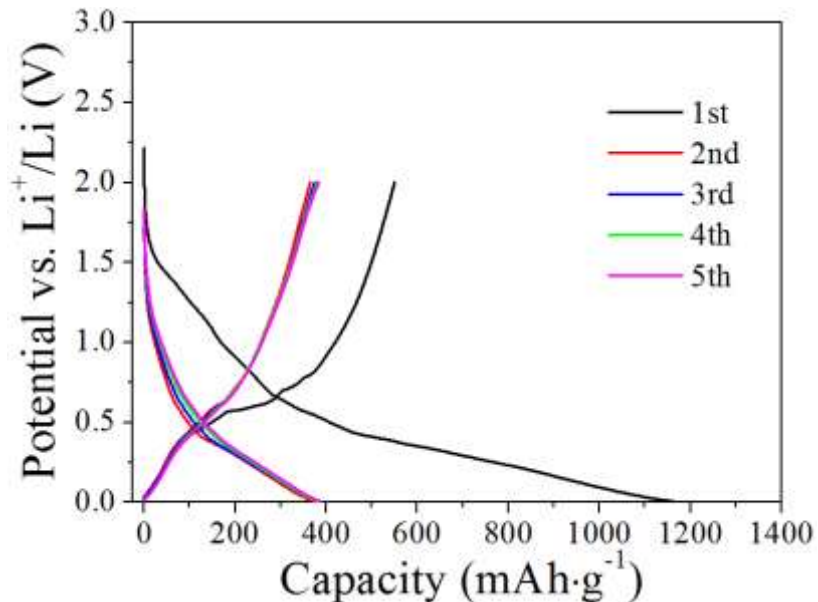


Figure S4. The CV curves of YSn₂-Ar at 0.1 mV s⁻¹.



FigureS5. The Nitrogen adsorption-desorption isotherm curves of Sn/YH_x.



FigureS6. The voltage profiles of YSn₂-Ar at 100 mA g⁻¹.

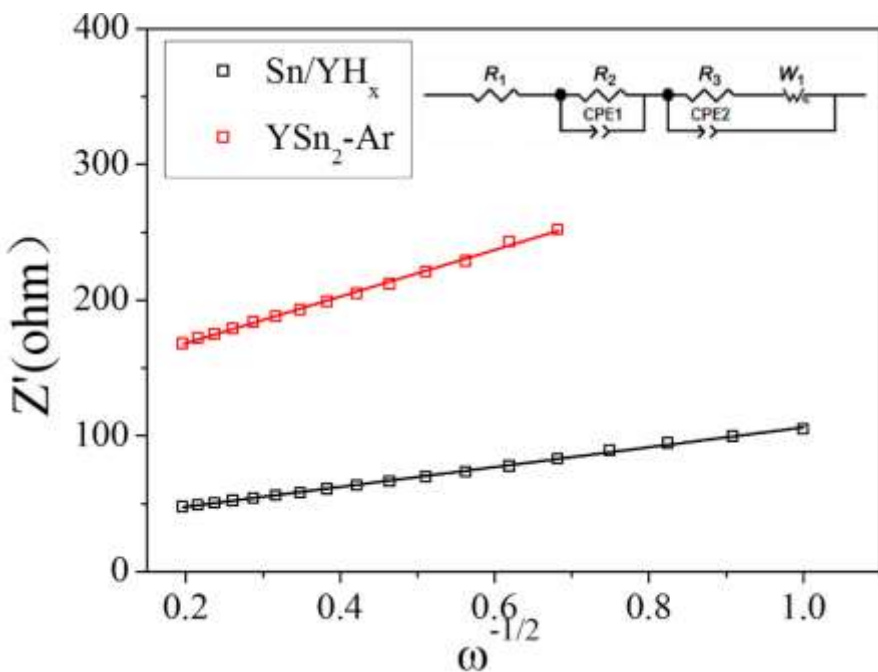


Figure S7. Plots of the real parts of the impedance (Z') versus the reciprocal square root of the angular frequency ($\omega^{-1/2}$) of Sn/YH_x and $\text{YSn}_2\text{-Ar}$ in the low frequency region after twenty cycles.

Table S1. Simulated EIS parameters of Sn/YH_x and $\text{YSn}_2\text{-Ar}$ after twenty cycles.

	$R_1(\Omega)$	$R_2(\Omega)$	$R_3(\Omega)$	σ
Sn/YH_x	3.85	35.04	15.3	73.05
$\text{YSn}_2\text{-Ar}$	4.73	125.10	152.0	172.75

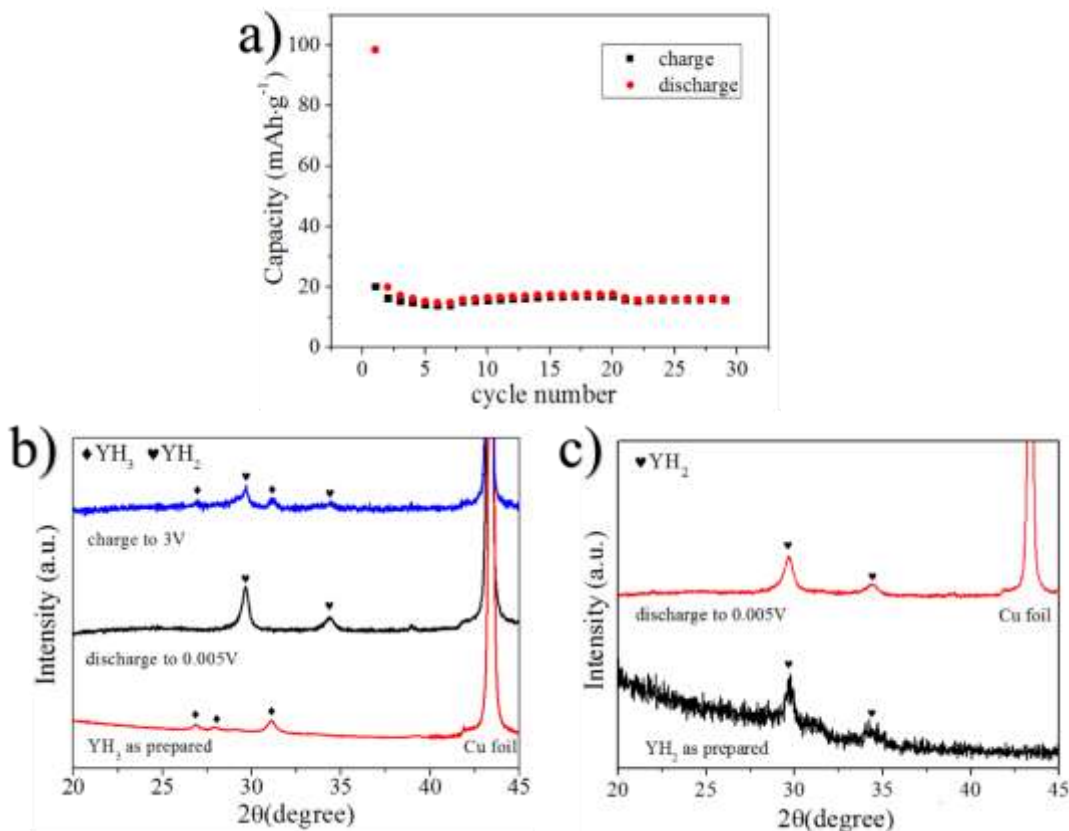


Figure S8. a) The capacity of pure YH₃, subtracting the capacity of carbon conductive agent, b) the XRD patterns of YH₃ during the 1st discharge/charge process, c) the XRD patterns of YH₂ during the 1st discharge/charge process

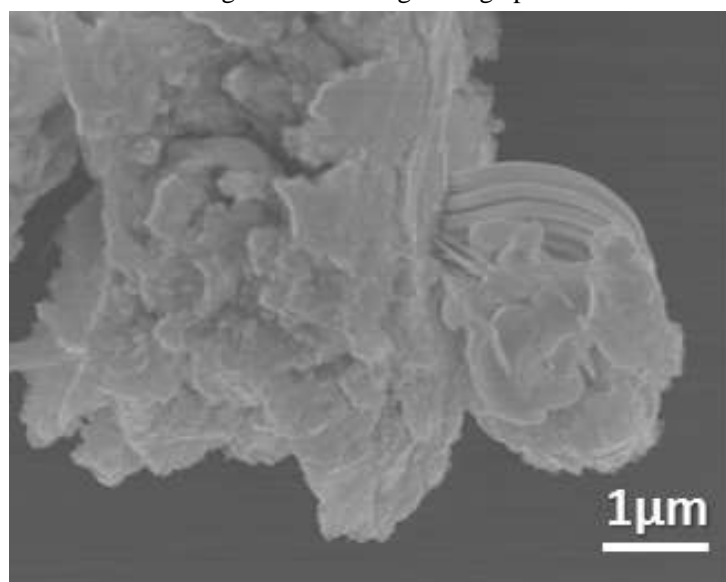


Figure S9. An SEM image of Sn/YH_x without carbon buffer agent.

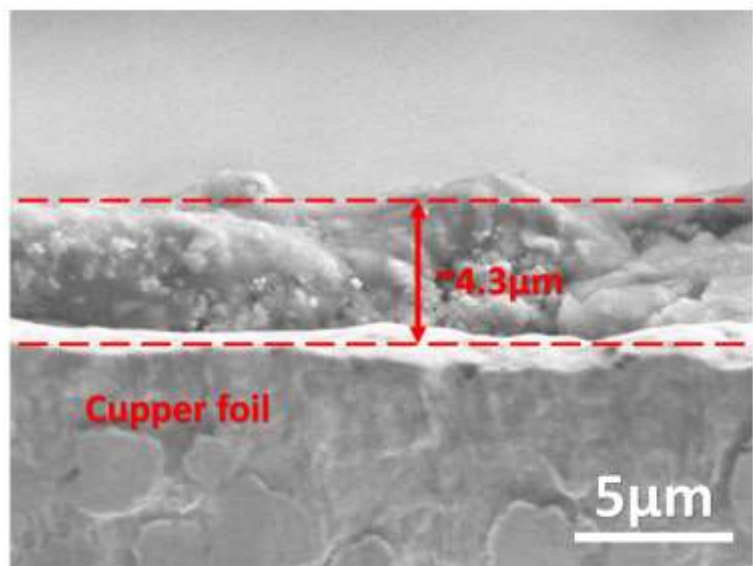


Figure S10. The thickness of electrode observed by SEM.

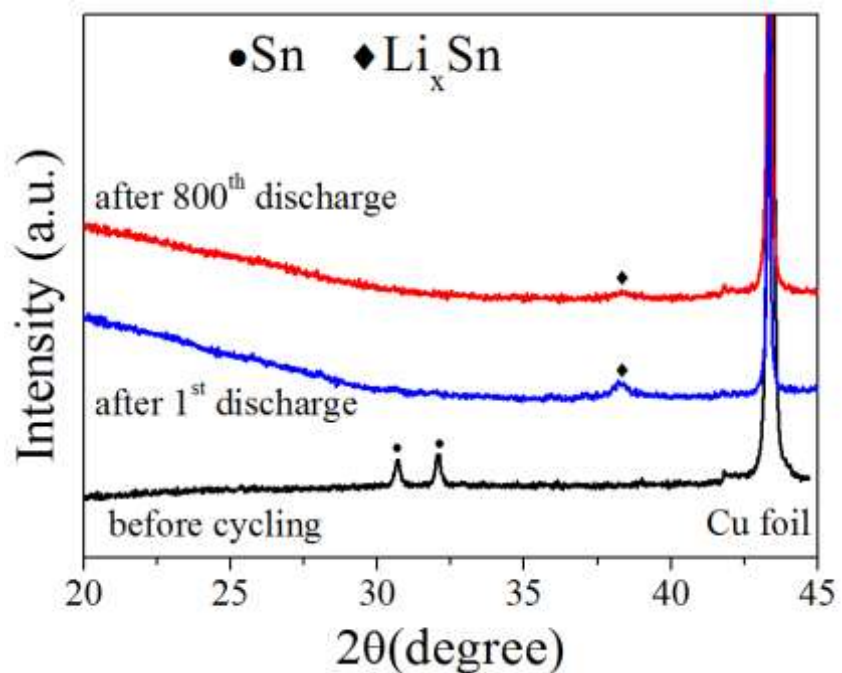


Figure S11. The XRD patterns of Sn/YH_x before and after cycling.

Table S2. Comparison of the capacity of Sn/YH_x with other Sn-based, Si-based and carbon-based anodes in LIBs reported in literature.

Materials	Volumetric capacity (mAh cm ⁻³)		Density (g cm ⁻³)		Gravimetric capacity (mAh g ⁻¹)	Cycles	Current density	Potential region	Mass loading (mg cm ⁻²)	Ref.
	active materials	electrode	active materials*	Electrode [#]						
Sn/YH _x	2594	1404	5.15	2.79	503.5	1000	500 mA g ⁻¹	0.005-2V	1.24	This work
PVP-Sn(IV)@Ti3C	1374.8	N/A	2.16	N/A	635	50	100 mA g ⁻¹	0.01-3V	N/A	1
Sn/C nanocomposite	1700	1700	1.92	1.92	885.4	200	0.5C	0.01-3V	N/A	2
SnO ₂ @GC-21	2123	1075	2.18	1.38	973.8	300	100 mA g ⁻¹	0.01-3V	1.87	3
C@Sn@C nanofibers	760	N/A	1.31	N/A	580	100	500 mA g ⁻¹	0.005-3V	N/A	4
Cu ₆ Sn ₅ -TiC-C	1340	N/A	2.197	N/A	610	60	100 mA g ⁻¹	0-2V	N/A	5
SnO ₂ @Si nanospheres	N/A	1030	N/A	1.326	778	500	300 mA g ⁻¹	0.01- 1.1V	1.7-1.8	6
Sn-Fe@C	N/A	N/A	N/A	N/A	441.6	100	100 mA g ⁻¹	0.01-2V	N/A	7
Sn-Fe	N/A	N/A	N/A	N/A	227.3	20	100 mA g ⁻¹	0.01-2V	N/A	8
LaSn ₃	N/A	N/A	N/A	N/A	200-250	20	200 mA g ⁻¹	0.0-1.5V	N/A	9
FeCuSi	N/A	2059	N/A	1.6	1287	50	0.5C	0.005-1V	N/A	10
3D Si membrane	429	429	0.167	0.167	2568.8	100	300 mA g ⁻¹	0.01- 1.5V	N/A	11
SiNP-PANi	1078	1078	0.899	0.899	1199.1	600	1000 mA g ⁻¹	0.01-1V	0.3	12
nano-Si SC	1725	1138	1.38	0.91	1250	1400	1C	0.01-1V	2	13
SG-Si-c-PAN	N/A	2350	N/A	0.85	2764.7	100	100 mA g ⁻¹	0.05- 1.5V	1.3-2.5	14
Si pomegranate	N/A	1270	N/A	0.4	3175	1000	C/2	0.01-1V	~0.2	15
SiNP-alginate	N/A	850	N/A	0.5	1700	100	4200 mA g ⁻¹	0.01-1V	N/A	16
Gr-Si-CNM	2821	2821	2.3	2.3	1226.5	1000	1800 mA g ⁻¹	0.01- 1.5V	0.07	17

Holey-graphene monolith	N/A	1052	N/A	1.1	956	1200	0.1 mA cm ⁻²	0.01-3V	2.75	18
Porous graphene/Co	358	N/A	0.398	N/A	900	300	50 mA g ⁻¹	0.01-3V	1-2	19
I-N-codoped carbon microspheres	1090	N/A	1.59	N/A	685	500	1 mA cm ⁻²	0.01-3V	N/A	20

* The density of the active material is calculated using the theoretical density of the components and the percentage of the component or the void in the active material, according to the literature.

The density of the electrode is given by either the tap density of the active material or by the density of the fabricated electrode (calculated by the mass of all the electrode material divided by the apparent volume of the material on the current collector), according to the literature.

The calculation of the density of Sn/YH_x material and the fabricated Sn/YH_x electrode is given as an example.

Calculation of the density of the Sn/YH_x composite and the fabricated Sn/YH_x electrode.

● The density of the Sn/YH_x composite

The hydrogenated system Sn/YH_x consists of metal Sn, YH_x and acetylene black (AB). The quantitative relationship among these three components is that the atomic ratio of Sn:Y is 1:2 and that the mass of AB is 10% of pristine YSn₂. We regard the density of YH₃ as the approximate value of YH_x. Considering the structure of Sn/YH_x is dense without any porous or voids after ball milling, the average density of Sn/YH_x can be represented as:

$$\rho_{\text{average}} = \frac{m_{\text{total}}}{V_{\text{total}}} = \frac{m_{\text{total}}}{\left(\frac{m_{\text{Sn}}}{\rho_{\text{Sn}}} + \frac{m_{\text{YH}_3}}{\rho_{\text{YH}_3}} + \frac{m_{\text{AB}}}{\rho_{\text{AB}}} \right)} = \frac{1}{\left(\frac{\omega_{\text{Sn}}}{\rho_{\text{Sn}}} + \frac{\omega_{\text{YH}_3}}{\rho_{\text{YH}_3}} + \frac{\omega_{\text{AB}}}{\rho_{\text{AB}}} \right)} \quad (\text{S1})$$

where ω_{Sn} , ω_{YH_3} and ω_{AB} are respectively the mass ratio of Sn, YH₃ and AB to the total mass, which can be easily calculated according to the quantitative relationship. The values are 65.59%, 25.39% and 9.02% respectively. The standard densities of Sn and YH₃ are respectively 7.28 g cm⁻³ and 3.97 g cm⁻³.²¹ The density of ball milled AB is approximately equal to density of graphite, which is 2.25 g cm⁻³.²¹ As these numbers replaced into Eq. (S1), the average density (ρ_{average}) is output immediately as 5.15 g cm⁻³.

● The density of the fabricated Sn/YH_x electrode

The mass load of the electrode is 1.2 mg cm⁻². The thickness of the electrode material on the copper foil is 4.3 μm. Thus, the density of the fabricated electrode is:

$$\rho_{\text{electrode}} = m/d \quad (\text{S2})$$

Where m is the mass load of the electrode, d is the thickness of the electrode material. As the number replaced into Eq. (S3), the density of the fabricated electrode is output immediately as 2.79 g cm⁻³.

The calculation details of GITT

To study the difference between lithium diffusion coefficient of Sn/YH_x and YSn₂-Ar under various potential, GITT is performed. The value of the Li diffusion coefficient D was calculated by Fick's second law of diffusion as Eq.S1:^{22, 23}

$$D = \frac{4}{\pi} \left(\frac{m_B V_M}{M_B S} \right)^2 \left(\frac{\Delta E_t}{\Delta E_1} \right)^2 \quad \left(\tau \ll \frac{L^2}{D} \right) \quad (\text{S3})$$

where D is the lithium diffusion coefficient, L is the diffusion distance, m_B is the mass of active material, M_B is the molar weight, V_M is the molar volume, S is the surface area of the electrode, ΔE_t

is the total change of potential during the discharge at constant current, ΔE_S is the change of the steady-state potential.

Reference

1. J. Luo, X. Tao, J. Zhang, Y. Xia, H. Huang, L. Zhang, Y. Gan, C. Liang and W. Zhang, *ACS Nano*, 2016, **10**, 2491-2499.
2. J. Liu, X. Chen, J. Kim, Q. Zheng, H. Ning, P. Sun, X. Huang, J. Liu, J. Niu and P. V. Braun, *Nano Lett.*, 2016, **16**, 4501-4507.
3. J. W. Han, D. B. Kong, W. Lv, D. M. Tang, D. L. Han, C. Zhang, D. H. Liu, Z. C. Xiao, X. H. Zhang, J. Xiao, X. Z. He, F. C. Hsia, C. Zhang, Y. Tao, D. Golberg, F. Y. Kang, L. J. Zhi and Q. H. Yang, *Nat. Commun.*, 2018, **9**, 9.
4. X. Wang, K. Gao, X. Ye, X. Huang and B. Shi, *Chem. Eng. J.*, 2018, **344**, 625-632.
5. D. Applestone and A. Manthiram, *RSC Adv.*, 2012, **2**, 5411-5417.
6. T. Ma, X. Yu, H. Li, W. Zhang, X. Cheng, W. Zhu and X. Qiu, *Nano Lett.*, 2017, **17**, 3959-3964.
7. H. Shi, A. Zhang, X. Zhang, H. Yin, S. Wang, Y. Tang, Y. Zhou and P. Wu, *Nanoscale*, 2018, **10**, 4962-4968.
8. S. Gao, A.-M. Wu, X.-Z. Jin, F. Ye, X.-L. Dong, J.-Y. Yu and H. Huang, *J. Alloy. Compd.*, 2017, **706**, 401-408.
9. J. T. Vaughey, M. M. Thackeray, D. Shin and C. Wolverton, *J. Electrochem. Soc.*, 2009, **156**, A536-A540.
10. S. Chae, M. Ko, S. Park, N. Kim, J. Ma and J. Cho, *Energy Environ. Sci.*, 2016, **9**, 1251-1257.
11. F. Xia, S. B. Kim, H. Cheng, J. M. Lee, T. Song, Y. Huang, J. A. Rogers, U. Paik and W. I. Park, *Nano Lett.*, 2013, **13**, 3340-3346.
12. H. Wu, G. Yu, L. Pan, N. Liu, M. T. McDowell, Z. Bao and Y. Cui, *Nat. Commun.*, 2013, **4**, 1943.
13. D. C. Lin, Z. D. Lu, P. C. Hsu, H. R. Lee, N. Liu, J. Zhao, H. T. Wang, C. Liu and Y. Cui, *Energy Environ. Sci.*, 2015, **8**, 2371-2376.
14. F. M. Hassan, R. Batmaz, J. Li, X. Wang, X. Xiao, A. Yu and Z. Chen, *Nat. Commun.*, 2015, **6**, 8597.
15. N. Liu, Z. Lu, J. Zhao, M. T. McDowell, H.-W. Lee, W. Zhao and Y. Cui, *Nat. Nanotech.*, 2014, **9**, 187.
16. I. Kovalenko, B. Zdyrko, A. Magasinski, B. Hertzberg, Z. Milicev, R. Burtovyy, I. Luzinov and G. Yushin, *Science*, 2011, **334**, 75.
17. S. Suresh, Z. P. Wu, S. F. Bartolucci, S. Basu, R. Mukherjee, T. Gupta, P. Hundekar, Y. Shi, T.-M. Lu and N. Koratkar, *ACS Nano*, 2017, **11**, 5051-5061.
18. X. P. Wang, L. X. Lv, Z. H. Cheng, J. A. Gao, L. Y. Dong, C. G. Hu and L. T. Qu, *Adv. Energy Mater.*, 2016, **6**, 7.
19. H. Cao, X. Zhou, W. Deng and Z. Liu, *J. Mater. Chem. A*, 2016, **4**, 6021-6028.
20. D. Wang, J. Zhou, J. Li, Y. Wang, L. Hou and F. Gao, *ACS Sustain. Chem. Eng.*, 2018, **6**, 7339-7345.
21. A. Jain, S. P. Ong, G. Hautier, W. Chen, W. D. Richards, S. Dacek, S. Cholia, D. Gunter, D. Skinner, G. Ceder and K. A. Persson, *APL Mater.*, 2013, **1**, 011002.
22. K. Yunok, M. Shoaib, K. Hyunchul, C. Yong-Hun, K. Hansu, K. J. Man and Y. Won-Sub, *Chem. Sus. Chem.*, 2015, **8**, 2378-2384.
23. C. J. Wen, B. A. Boukamp, R. A. Huggins and W. Weppner, *J. Electrochem. Soc.*, 1979, **126**, 2258-

2266.